Compensated Medium Voltage 6-Pulse CSR Using Shunt Active Power Filters: Three Different Configurations

MS Hamad[a] and MI Masoud*[b]

[a] Electrical Engineering Department, Arab Academy for Science and Technology, Alexandria, Egypt
*[b] Electrical and Computer Engineering Department, College of Engineering, Sultan Qaboos University, PO Box 33, PC 123, Al-Khoud, Muscat, Sultanate of Oman

Received 27 March 2013; accepted 2 July 2013

Abstract: The 6-pulse controlled AC/DC converter produces harmonics. The input current total harmonic distortion and the input power factor, which is firing delay angle dependent, are major drawbacks, and a compensation technique is mandatory. This paper introduces a compensated 6-pulse current source-controlled rectifier with a shunt active power filter (*APF*) in different configurations. The shunt *APF* with predictive current control is coupled to the 6-pulse systems in three different compensation configurations. The *APF* is connected either directly to the front-end transformer primary or secondary side or via a transformer to reduce the filter side voltage. The comparison between these configuration is introduced; each configuration has merits and demerits. The comparison cannot be genuine. Simulation results are presented for a medium voltage converter which is scaled to allow low-voltage experimental confirmation.

Keywords: Shunt active filter, 6-pulse converter, Medium voltage, Predictive current control, and Harmonics.

مقوم مصدر تيار للجهد المتوسط بعرض ست نبضات يعوض بمرشحات قوي متوازية فعالة: دراسة ثلاثة تكوينات مختلفة

مصطفى حمد و محمود مسعود*

الملخص: المقومات التى تحول من تيار ثابت إلى تيار متردد تنتج توافقيات. معامل التشوه لتيار الدخل و معامل القدرة تعتمدان على زاوية الإشعال والتي تعتبر من سلبيات هذه الأنظمة و خصوصا تأثيرها على تيار الدخل ولهذا نظام التعويض ضروري. هذه المقالة تقدم نظاماً مقوماً لمصدر تيار جهد متوسط بعرض ست نبضات مع وجود مرشحات قوية فعالة متوازية في تكوينات مختلفة. يتم التحكم في شكل التيار بنظام تحكم بالتنبؤ في الثلاثة تكوينات المطروحة. المرشح إما أن يتم تركيبه للجزء الابتدائي من المحول أو في الجزء الثانوي مباشرة أو من خلال محول يقلل جهد المرشح. يتم تقديم دراسة مقارنة بين هذه التكوينات؛ إذ أن كل تكوين له مزايا و عيوب و من خلال هذه المقارنة لا يمكن تحديد نظام يكون الأمثل على المطلق ولكن توجد عوامل يتم على أساسها اختيار النظام المطلوب. تم تقديم نمذجة للتكوينات لنظام الجهد المتوسط وتم تأكيدها عملياً بنظام مماثل بجهد منخفض.

الكلمات المفتاحية: مرشحات متوازية فعالة، مقوم ست نبضات ، الجهد المتوسط ، تحكم تنبؤي ، التوافقيات.

*Corresponding author's e-mail: m.masoud@squ.edu.om

1. Introduction

The 6-pulse phase controlled AC/DC converter is often employed in low voltage (*LV*) and medium voltage (*MV*) systems for domestic and industrial applications (Wu 2006; Freitas *et al*. 2007; Rice 1994). Although controlled converters could be a good choice for higher power applications, due to their high efficiency and reliability (Wiechmann *et al*. 2008) they have major drawbacks in terms of *AC* side power quality, input current total harmonic distortion (THD) and power factor (*pf*) (Bose 2009). The *AC* side harmonics occur at 6p ± 1 times the fundamental (p = 1, 2, 3…etc.). The magnitude of these harmonics and the overall *THD* do not meet input current *THD* standard guidelines (Williams online). Moreover, the power factor depends on the current *THD* and the thyristor firing delay angle (α) (Rashid 2001).

$$THD = \frac{\sqrt{I_s^2 - I_{s1}^2}}{I_{s1}} = 31.1\ \% \qquad (1)$$

Where, I_s is the root mean square (*RMS*) supply current and I_{s1} is the *RMS* fundamental supply current. The power factor can be calculated as:

$$pf = \frac{DPF}{\sqrt{1+THD^2}} = 0.955\cos\alpha \qquad (2)$$

Where, *DPF* is the displacement power factor, given by

$$DPF = \cos\alpha \qquad (3)$$

Higher pulse configurations are possible (Choi and Cho 2000; Hamad *et al*. 2012), but the system cost and complexity are increased and the problem of power factor dependency on the firing delay angle remains (Wu 2006). A compensating technique is therefore mandatory to compensate for both the reactive and harmonic currents in order to improve the input current THD and *pf* (Bose 2002). *APF* avoids passive filter drawbacks; moreover, it is durable and reliable (El-Habrouk *et al*. 2000; Akagi 1996; Akagi 2005; Rahmani *et al*. 2010; Singh and Solanki 2009).

In this paper, the 6-pulse converter is fed from a star/star front-end step-down transformer. Three *APF* connection configurations are considered, all with the objective of producing sinusoidal supply currents with a near unity power factor. In reference (Akagi *et al*. 1986), the *APF* is connected across the primary side. In the other configurations, the *APF* is connected via a high-bandwidth step-down transformer (Cheng *et al*. 1999). The *APF* is connected across the secondary side of the transformer (Tenca and Lipo 2004). For *MV* applications, reducing the filter side voltage affects the system size, losses, and cost, and permits a higher switching frequency (Akagi 2005). The three compensation connections to be compared are:

- The *APF* connected to the primary side,
- The *APF* connected directly to the secondary side, and
- A secondary side connection via a high-bandwidth step-down transformer.

The *APF* is controlled to compensate the main current *THD* and *pf*. Simulations for a *MV* system plus a scaled *LV* practical system are used to enable performance comparison of the three configurations.

The voltage source inverter (*VSI-APF*) is used as it is more convenient for *APF* applications since it is lighter, cheaper, and expandable to a multilevel configuration to improve the performance at high power compensation with lower switching frequencies (Routimo *et al*. 2007). Also, in this paper, *APF* operation is based on the control strategy (Hamad *et al*. 2012; Massoud *et al*. 2004a) where harmonic and reactive current extractions are achieved using capacitor voltage control (Anuradha and Kothari 1998; Huang and Wu 1999), and the current control is achieved using predictive control. This control technique is simple, suitable for *DSP* implementation, and provides a constant switching frequency (Massoud *et al*. 2004b). The design details of *APF* are introduced in (Hamad e*t al*. 2012).

After the introduction, the paper is organized as follows: Section 2 explains the compensation of a 6-pulse converter using a shunt *APF*. Section 3 introduces configuration #1. Section 4 introduces configuration #2. Section 5 introduces configuration #3. Finally, there is a discussion and conclusion.

2. The 6-Pulse Converter Compensated for with a Shunt APF

For *MV* voltage applications, reducing the filter side voltage greatly affects system size and cost, and allows a higher switching frequency. The lower phase voltage requirement of a star connected primary is exploited, which is important in *MV* applications. Typical parameters for the *MV* transformer and the operating system parameters used in the simulations are listed in Appendix 1. A 2 kVA, 415 V, 6-pulse scaled prototype converter was used to investigate the performance of the different *APF* configurations. The operating conditions are common for all tested configurations; v_s = 170 V, I_{dc} = 1A (switching devices are rated to 3A),

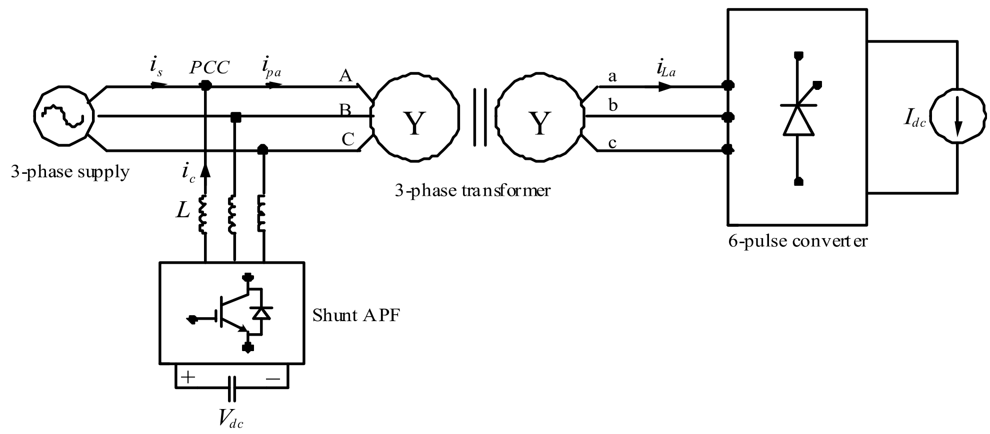

Figure 1. Configuration # 1 APF connected to the primary side.

f_{sw} = 3.6 kHz and C = 3.2 mF. The star/star windings of the prototype front-end transformer with parameters listed in Appendix 2 has a turns ratio of $N_1 / N_2 = 2$. The operational environment is:

- A three-phase, three-wire system
- A balanced and sinusoidal voltage supply
- A negligible source impedance, and
- A balanced harmonic current-producing load.

All simulations and practical results are recorded for the representative phase '*a*', as the system is a balanced three-phase one.

3. Configuration # 1

In Fig. 1, the shunt *APF* is connected to the primary side of the front-end Y-Y transformer. The objective was to produce a sinusoidal supply current with near unity power factor. The *APF* inverter *DC* side voltage (V_{dc}) determines the voltage rating of the shunt *APF* switches, where V_{dc} is greater than the line peak voltage at the point of common coupling (*PCC*). For a *MV* system, the inverter requires semiconductor devices with high voltage ratings, possibly involving the series connection of switching devices.

3.1 Simulation Results

A *MATLAB/Simulink* (MathWorks, Inc., Natick, MA, USA) model of the *MV* compensated 6-pulse converter was used to study the effect of the shunt *APF* on the system performance. The simulation models the supply as sinusoidal, balanced, or having negligible impedance. The capacitor voltage was controlled at 7.6 kV. Figure 2 shows the simulation results of parts *a-f* when the 6-pulse converter operates at zero delay ($\alpha = 0$) and the *APF* is connected to shown *PCC*. The supply phase voltage (v_s) is shown in part a. The primary current (i_p) is shown in *b*, while *c* shows the compensating current (i_c) injected by the *APF*. The supply current (i_s) shown in d became sinusoidal after activation of the *APF* as the compensating current cancels the current harmonics in ip produced by the 6-pulse converter. Parts *e* and *f* show the supply current frequency spectra before and after compensation. No triplen components arise in a balanced three-phase system.

3.2 Practical Results

The *LV* prototype system representing configuration #1 was tested experimentally, with a 12 mH, 3-phase interfacing inductor and the capacitor DC-voltage controlled at 400 V. The test was performed with the converter operating in the rectifier mode (α = 0-90°). Parts a-c of Fig. 3 show the experimental results when the converter operates with α = 45. Part a shows that the harmonic and reactive current components of the front-end transformer ip were compensated for by the filter current (i_f). The compensated is sinusoidal and in phase with the v_s. The spectra of the practical recorded supply current before and after activating the *APF* are shown in *b* and *c*, respectively. The *THD* improved from 28.5% to 13.4%, and the power factor improved from 0.6 to 0.912.

3.3 Discussion

Configuration #1 achieved the target of sinusoidal supply current with a near unity power factor, but may not be suitable for *MV* applications because the *APF* was connected directly to the front-end *MV* transformer primary. Consequently, the *MV* inverter capacitor is large and costly. The filter bandwidth was limited as was the switching frequency due to the high voltage, possibly comprised of series connected semiconductor devices, which increases control complexity, filter size and cost. To overcome these voltage problems, the *APF* can be coupled to the *PCC* via a high-bandwidth, *MV* transformer, but the costs would be

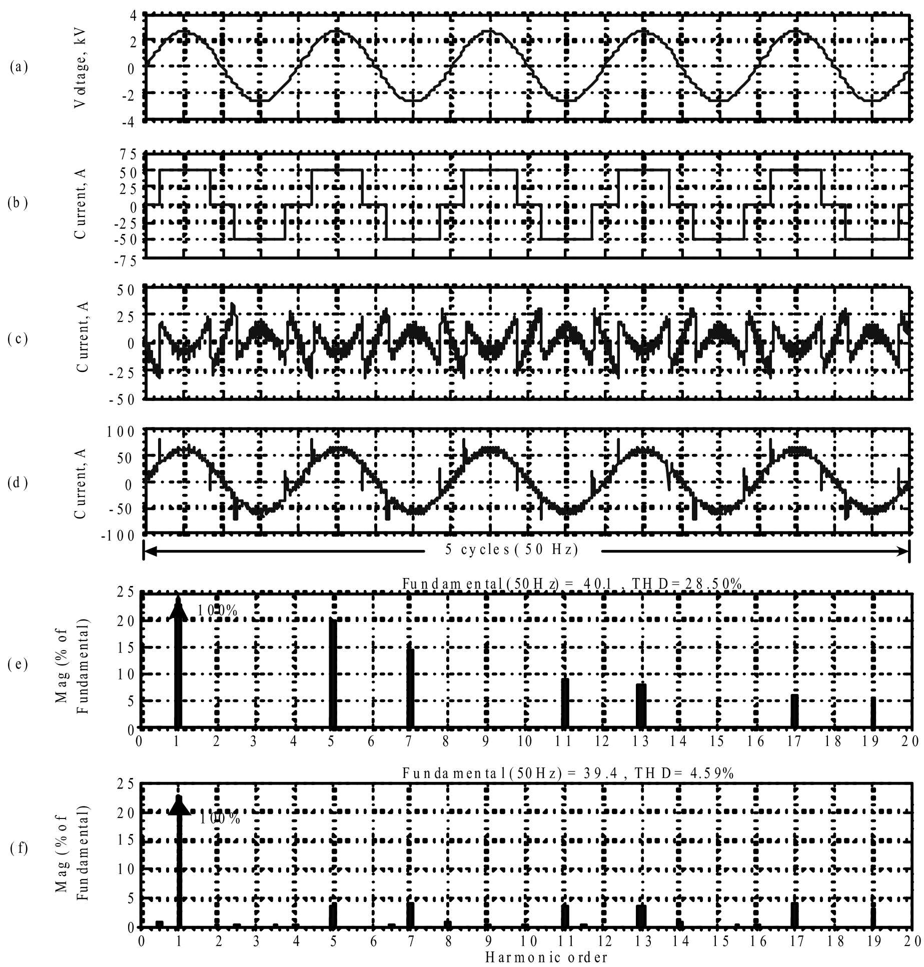

Figure 2. Configuration #1 at $\alpha = 0°$: (a) supply phase voltage, v_s, (b) transformer primary current, i_p, (c) filter current, i_c, (d) compensated supply current, i_s, (e) spectrum of converter current, and (f) spectrum of compensated supply current.

high (Corasniti *et al.* 2008). The transformer ratings increase due to the transmission of the harmonics and reactive current. An alternative solution would be to connect the *APF* to the front-end transformer secondary side.

4. Configuration # 2

APF is connected to the front-end transformer secondary as shown in Fig. 4. The same control concept is applied to all configurations, while it is detailed here for configuration #2. The transformer secondary phase voltages and currents were measured and used in the control system. The turns ratio of the front-end transformer is $N_1 / N_2 = 2$; thus, the voltage at the *PCC* was half that of configuration #1. This means that the capacitor voltage can be controlled at a lower voltage; consequently, semiconductor devices with a lower voltage rating can be used and, therefore, the operating switching frequency limit and the filter bandwidth can both be increased. The filter-side current was doubled. A device voltage rating reduction only can be achieved if a step down transformer is used.

4.1 Simulation Results

The MATLAB model for the *MV* 6-pulse converter was modified to study the compensation technique using configuration #2. The voltage reduction at the *PCC* required a change to some of the operating parameters, as listed in Appendix 3. The simulation results for $\alpha = 45$ are shown in Fig. 5. The secondary phase voltage was measured then scaled to synchronize the secondary reference current (i^*_{sec}). The supply phase voltage is shown in Fig. 5a. The converter current (i_L) is shown in Fig. 5b and the injected *APF* current is shown in Fig. 5c and compensates the harmonic and reactive currents.

The resulting sinusoidal transformer secondary current (i_{sec}) is shown in Fig. 5d. By transformer action, i_{sec} was transformed to the primary side. The primary current was the supply current (i_s) as shown in *e*. The supply current was sinusoidal and in phase with the

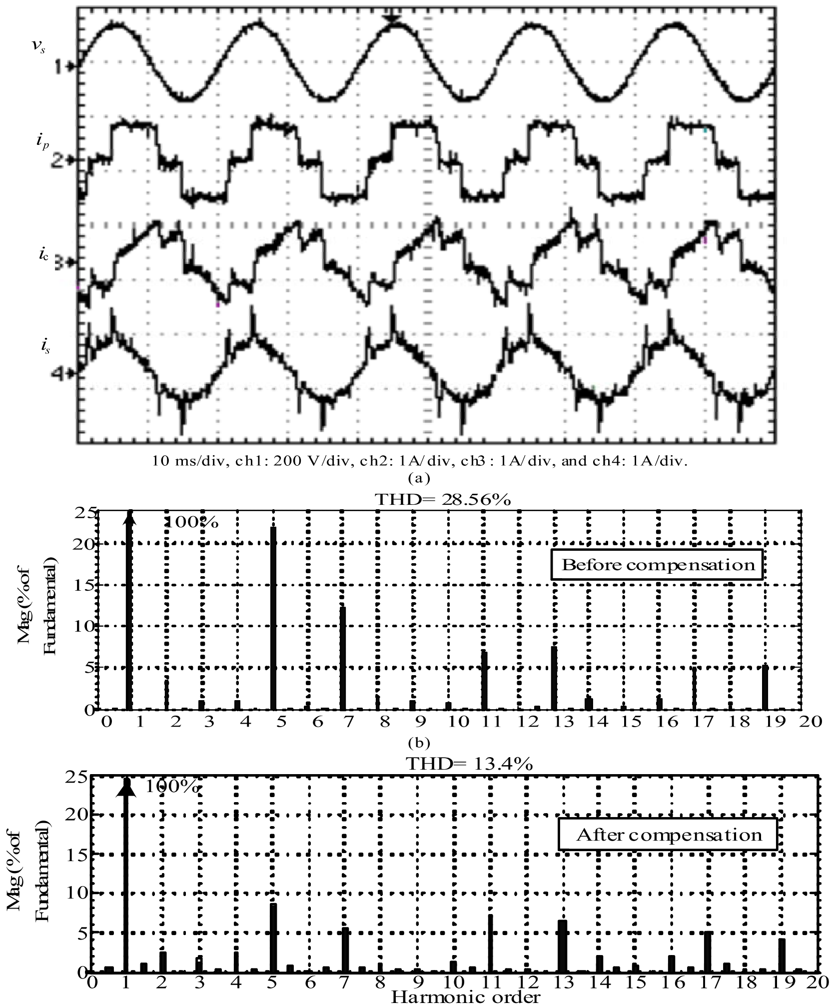

Figure 3. Configuration #1 practical results at $\alpha = 45^o$: (a) current waveforms, and (b) & (c) supply current spectrum before and after compensation, respectively.

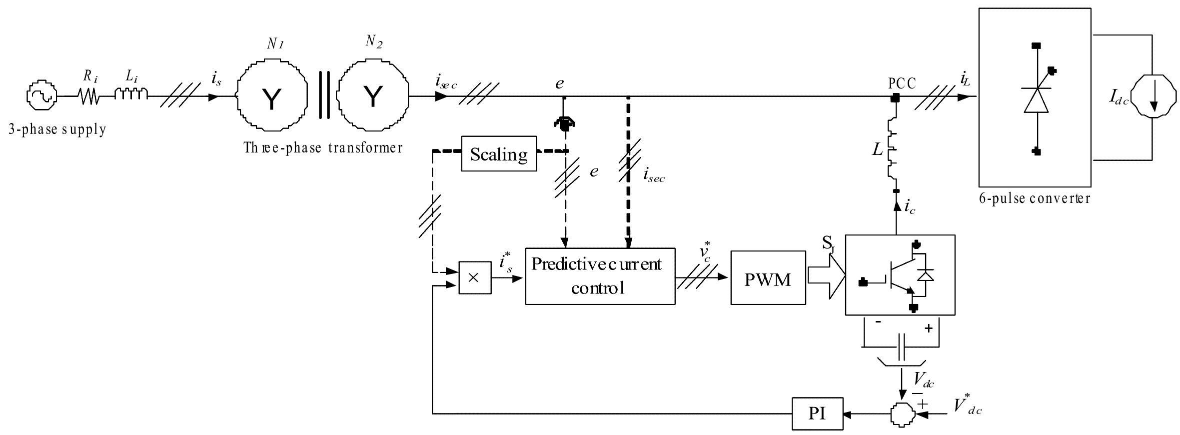

Figure 4. Configuration #2 APF on the secondary side.

supply phase voltage. The spectra of the compensated i_{sec} and are shown in Figs. 5f and 5g, respectively. From the simulation results, it can be observed that the *MV* transformer had a negligible effect on the compensated system performance, as the *THD* of i_{sec} and i_s were virtually the same as what can be seen in configuration #1. The achieved input power factor (0.992 lagging) indicates that reactive power was absorbed by the transformer. However, the *RMS* filter current increases from 41.2 A, (configuration #1), to 66.5 A, (configuration #2). With the same inverter switching frequency, the same performance was achieved for both configurations, but with a lower voltage rated *APF*. Compensation on the secondary avoided har-

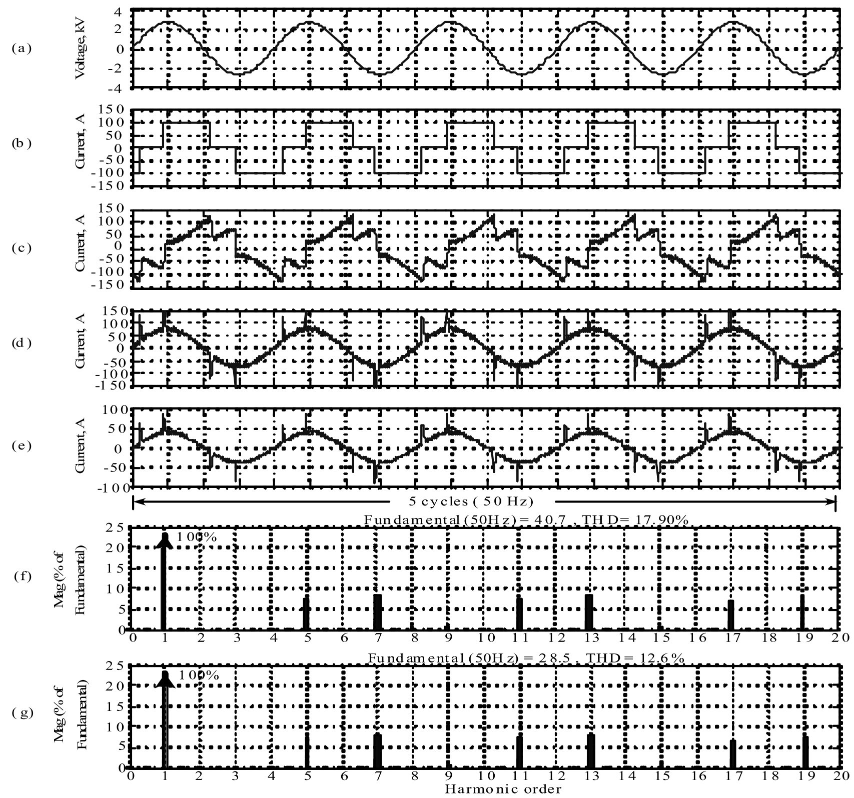

Figure 5. Configuration #2 for α = 45º; (a) supply phase voltage, v_s, (b) converter current, i_t, (c) filter current i_s, (d) compensated secondary current, i_{sec}, (e) compensated supply current, i_{sec}, (f) spectrum of i_{sec}, (g) spectrum of i_s.

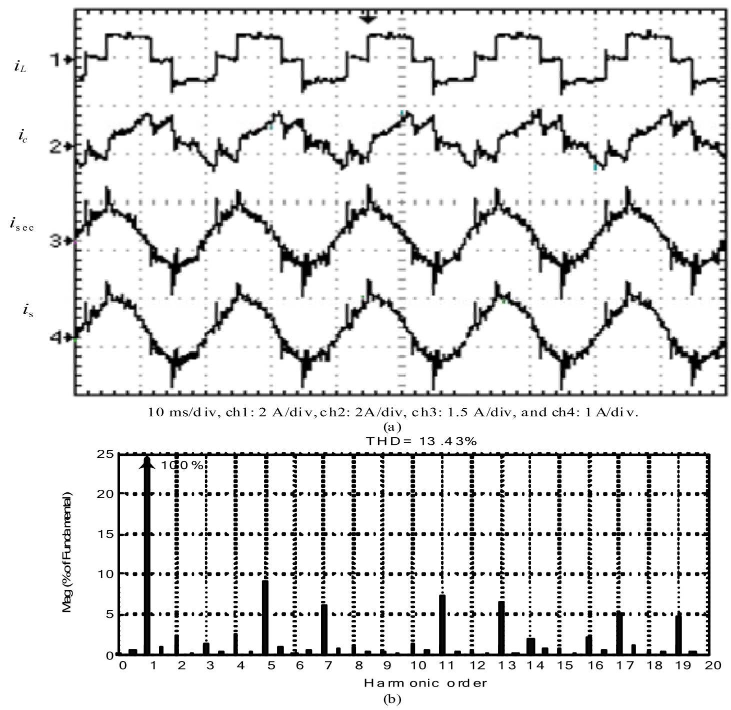

Figure 6. Configuration #2 practical results at α=45º: (a) current waveforms and (b) spectrum of compensated supply current i_s.

monic and the reactive currents passing through the transformer; consequently, the transformer harmonic burden was reduced.

4.2 Practical Results

Three-phase secondary side interfacing inductors of 5 mH were used and the capacitor voltage was con-

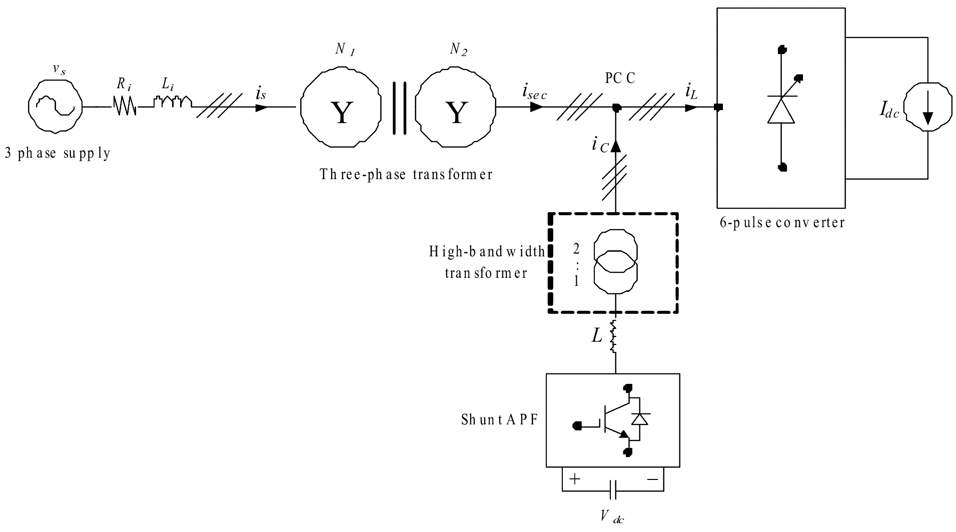

Figure 7. Configuration #3 APF in the secondary side with a high quality stepdown transformer.

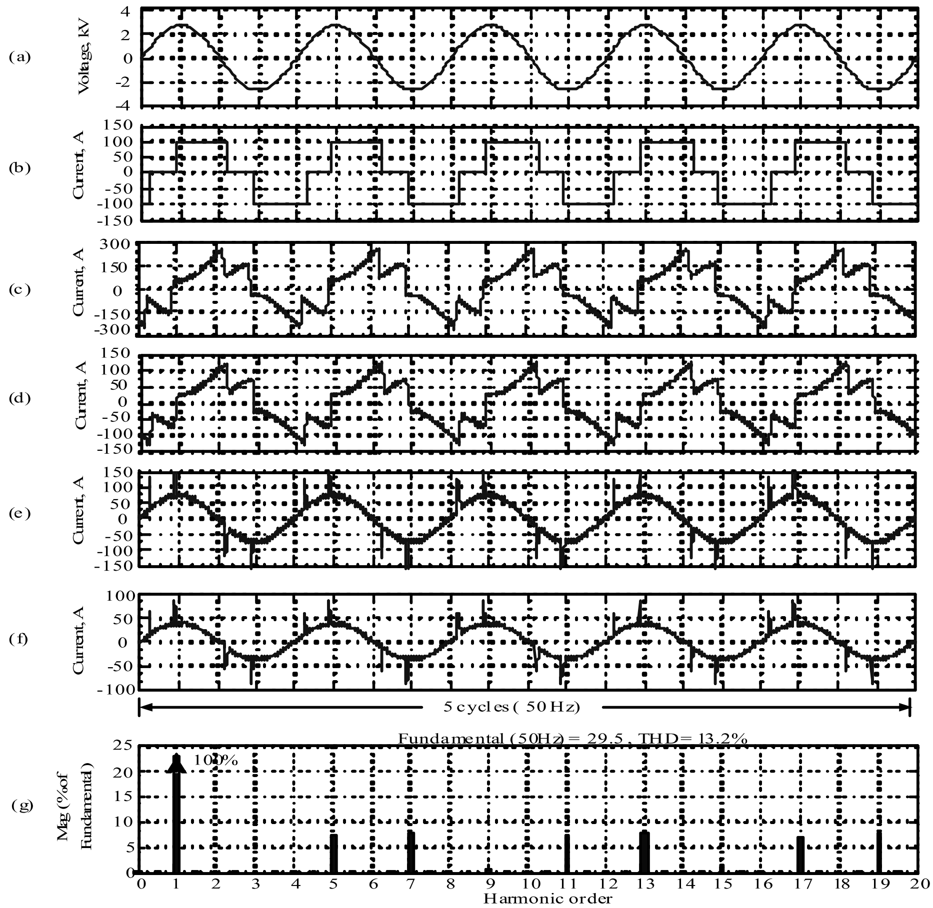

Figure 8. Configuration #3 at α=45º; (a) supply phase voltage, v_s, (b) converter current, i_t, (c) filter current, i_f, (d) compensation current, i_c, (e) compensated secondary current, i_{sec}, (f) compensated supply current, i_s, (g) spectrum of compensated supply current.

trolled at 220V. The experimental results for α = 45 are shown in part Fig. 6a. The i_f compensated for the i_L, resulting in the isec and, consequently, the i_s was compensated for. The spectrum of the practical recorded supply current after activating the *APF* is shown in Fig. 6b. The *THD* was improved from 28% to 13.43% and the power factor was improved from 0.6 to 0.92 lagging.

Table 1. Configuraton performance before compensation.

Configuration	Firing angle α	Primary current Fundamental rms (A)	*THD* %	Power factor lagging	Input power (kW)	i_T (A)
1	0°	40.1	25.5	0.955	218.89	-
	45°	41.6	26.5	0.60	133.15	-
2	0°	40.1	25.5	0.955	218.89	-
	45°	40.7	25.2	0.60	139.6	-
3	0°	39.6	28.5	0.956	216.38	-
	45°	39.6	26	0.59	126.75	-

Table 2. Configuration performance after compensation.

Configu-ration	Firing angle α	Primary current Fundamental rms (A)	*THD* %	Power factor Lagging	Input power (kW)	Filter current rms (A)	i_T (A)
1	0°	39.4	4.6	0.99	223.4	11.7	-
	45°	28.7	12.8	0.99	162.7	41.8	-
2	0°	39.5	4.6	0.99	224	23.2	-
	45°	28.5	12.6	0.99	162	66.5	-
3	0°	39.5	4.3	0.99	227	46.5	-
	45°	29	13.2	0.99	171	124.5	-

5. Configuration # 3

Filter side voltage reduction can be achieved by using the transformer coupling configuration shown in Fig. 7. As a case study, the turns ratio of the high bandwidth APF transformer was 2:1. This stepped down the PCC voltage to 825V and allowed the interfacing inductance to be reduced from 5 mH to 2 mH. The switching frequency was 3.6 kHz and the capacitor voltage was controlled at a reduced voltage of 1.8 kV (3.7 kV in configuration #2). The simulation results for α = 45 are shown in Figs. 8a-f. The front-end transformer secondary phase voltage was used to extract the i_{sec}^*. The supply phase voltage, the converter current, i_L, and the i_f, are shown in parts Figs. 8a-c, respectively. The *MV*-side of the *APF* transformer i_c is shown in Fig. 8d. The filter *RMS* current was 124.5 A. The i_{sec} is shown in Fig. 8e. The compensated secondar current is shown in Fig. 8f and was sinusoidal and in phase with the supply phase voltage. The spectrum of the compensated supply current is shown in Fig. 8g. This control system achieves 29A of the *RMS* fundamental supply current and a *THD* of 13.2% with an input power factor of 0.991 lagging. The capacitor voltage was controlled at half the voltage of configuration #2 but the filter current was doubled as a result of utilizing the *APF* 2:1 high-bandwidth step-down transformer.

The matching transformer core material was required of being capable of transmitting the highest required harmonic compensating component frequency.

6. Conclusions

The *APF* used in three different configurations compensated both the supply current and input power factor of a 6-pulse converter system. Configuration #1 is restricted to *MV* applications as the operating voltage of the *APF* inverter semiconductor switches and the switching frequency are limited. Configurations 2 and 3 overcome the voltage problem as the compensation is on the secondary side of the front end transformer. All the configurations achieve virtually the same supply current *THD* and the *pf* is improved to near unity. Configuration 3 offers reduced voltage stresses on the semiconductor devices but the filter current is doubled with respect to configuration #2. Table 1 shows the configuration performances before compensation while Table 2 shows the configuration performance after compensation. The *THD* follows the standard at zero firing angle however, if the firing angle is bigger than zero the *THD* is increased by nature even the system is compensated. The selection of the *APF* position depends on voltage level and user. No clear conclusion can be made about which configuration is the best. If the voltage needs to be reduced than configuration #1 is not suitable. If there is no problem with switches current and voltage is required to be lower, configuration 3 is the preferred choice.

References

Akagi H, Nabae A, Atoh S (1986), Control strategy of active power filters using multiple voltage-source PWM converters. Transaction on IEEE Industrial Applications 22(3):460.

Akagi H (1996), New trends in active filters for power conditioning. Transactions on IEEE Industry Applications 32(6):1312-1322.

Akagi H (2005), Active Harmonic Filters. Proceedings of the IEEE 93(12):2128-2141.

Anuradha BS, Kothari DP (1998), Analysis of a novel active filter for balancing and reactive power compensation. IEE Conference on Power Electronics and Variable Speed Drives 456:57-62.

Bose BK (2002), Modern power electronics and AC drives. Prentice Hall, Upper Saddle River.

Bose BK (2009), Power electronics and motor drives recent progress and perspective. Transactions on IEEE Industrial Electronics 56(2):581-588.

Cheng PT, Bhattacharya S, Divan DM (1999), Application of dominant harmonic active filter system with 12 pulse nonlinear loads. Transactions on IEEE Power Delivery 14(2):642-647.

Choi S, Oh J, Cho J (2000), Multi-pulse converters for high voltage and high power applications. Third International Power Electronics and Motion Control Conference IPEMC 2000 (3):1019-1024.

Corasaniti VF, Barbieri MB, Arnera PL, Valla MI (2008), Comparison of active filters topologies in medium voltage distribution power systems. Power and Energy Society General Meeting - Conversion and Delivery of Electrical Energy in the 21st Century: 1-8.

El-Habrouk M, Darwish MK, Mehta P (2000), Active power filters: A review. IEEE Proceeding on Electric Power Application 147(5):403-413.

Freitas LCG, Simoes MG, Canesin CA, Freitas LC (2007), Performance evaluation of a novel hybrid multipulse rectifier for utility interface of power electronic converters. Transactions on IEEE Industrial Electronics 54(6):3030-3041.

Hamad MS, Masoud MI, Finney SJ, Williams BW (2012), Medium voltage 12-pulse converter: AC side compensation using a shunt active power filter in a novel front end transformer configuration. Transaction on IET Power Electron 5:1315-1323.

Huang SJ, Wu JC (1999), A control algorithm for three-phase three-wired active power filters under non-ideal mains voltages. Transaction on IEEE Power Electronics 14:153-760.

Massoud[a] AM, Finney SJ, Williams BW (2004), Predictive current control of a shunt active power filter. 35th IEEE Power Electronics Specialists Conference, Aachen. Germany PESC'04:7803-8399.

Massoud[b] AM, Finney SJ, Williams BW (2004), Review of harmonic current extraction techniques for an active power filter. 11th International Conference on Harmonics and Quality of Power:154-159.

Rahmani S, Mendalek N, Al-haddad K (2010), Experimental design of nonlinear control technique for three-phase shunt active power filter. Transactions on IEEE Industrial Electronics 57(10):3364-3375.

Rashid MH (2001), Power Electronics: Handbook. Academic Press, Canada.

Rice DE (1994), A detailed analysis of six-pulse converter harmonic currents. Transactions on IEEE Industry Applications 30(2):294-304.

Routimo M, Salo M, Tuusa H (2007), Comparison of voltage-source and current-source shunt active power filters. Transactions on IEEE Power Electronics 22(2):636-643.

Singh B, Solanki J (2009), An implementation of an adaptive control algorithm for a three-phase shunt active filter. Transactions on IEEE Industrial Electronics 56(8):2811-2820.

Takeda M, Ikeda K, Teramoto A, Htsuka T (1988), Harmonic current and reactive power compensation with an active filter. IEEE Power Electronics Specialists Conference, PESC 88:1174-1179.

Tenca P, Lipo TA (2004), Reduced cost current-source topology improving the harmonic spectrum through on-line functional minimization. 35th IEEE Power Electronics Specialists Conference, PESC'04 (4):2829-2835.

Wiechmann EP, Aqueveque P, Burgos R, Rodriguez J (2008), On the efficiency of voltage source and current source inverters for high-power drives. Transactions on IEEE Industrial Electronics 55(4):1771-1782.

Williams BW [Online]. Power Electronics: Devices, Drivers, Applications, and Passive Components. Available eee.strath.ac.uk/~bwwilliams/book.htm.

Wu B (2006), High-Power Converters and AC Drives. Wiley-IEEE Press.

Appendix

Appendix I: *MV* transformer parameters.

Parameter	Value
Rated kVA	250 kVA
Primary/secondary Voltage	3.3/1650 kV
R_1 or R'_2 (pu)	0.005
X_1 or X'_2 (pu)	0.01
X_m (pu)	75
R_m (pu)	100

Appendix II: Prototype transformer parameters.

Parameter	Value
Rated kVA	2 kVA
Primary/secondary Voltage	420/210 V
R_1 (pu)	0.02
X_1 (pu)	0.02
R'_2 (pu), for a_t = 50 %	0.009
X'_2 (pu), for a_t = 50 %	0.023
X_m (pu)	22
R_m (pu)	102

Appendix III: *MV* system operating parameters.

System parameters	Configuration #1	Configuration #2	Configuration #3
PCC voltage, v_{ab}	3.5 kV	1.65 kV	825 V
Load current, I_{dc}	100 A	100 A	100 A
Interfacing inductance, L	12 mH	5 mH	2 mH
DC side capacitance, C	5 μF	5 μF	5 μF
Switching frequency, f_{sw}	3.6 kHz	3.6 kHz	3.6 kHz
Capacitor voltage	7.6 kV	3.7 kV	1.8 kV